crystallization communications

Expression, purification and preliminary crystallographic analysis of the *Toxoplasma gondii* enoyl reductase

Stephen P. Muench,[a] Sean T. Prigge,[b] Liqun Zhu,[b] Michael J. Kirisits,[c] Craig W. Roberts,[d] Sarah Wernimont,[c] Rima McLeod[c] and David W. Rice[a]*

[a]The Krebs Institute for Biomolecular Research, Department of Molecular Biology and Biotechnology, University of Sheffield, Firth Court, Western Bank, Sheffield S10 2TN, England, [b]Department of Molecular Microbiology and Immunology, Johns Hopkins Bloomberg School of Public Health, Baltimore, MD 21205, USA, [c]Department of Ophthalmology and Visual Sciences, Paediatrics, (Infectious Diseases) and Pathology and the Committees on Molecular Medicine, Genetics, Immunology and The College, The University of Chicago, Chicago, IL 60637, USA, and [d]Department of Immunology, University of Strathclyde, Glasgow G4 0NR, Scotland

Correspondence e-mail: d.rice@sheffield.ac.uk

The protozoan parasite *Toxoplasma gondii* is the causative agent of one of the most widespread parasitic infections of man and is a leading cause of congenital neurological birth defects and the third most common cause of food-borne deaths in the United States. Despite this, to date no drugs are available that provide a fully effective treatment. Recently, the antibacterial agent triclosan was shown to inhibit the fatty-acid biosynthesis pathway in *T. gondii* and to interact with the enoyl reductase (ENR). In order to analyse the potential of triclosan as a lead compound targeting *T. gondii* ENR and to explore unique features of the apicomplexan enzyme that could be exploited in future drug development, structural studies have been initiated on *T. gondii* ENR. Crystals of *T. gondii* ENR in complex with NAD$^+$ and triclosan were grown using the hanging-drop vapour-diffusion method with PEG 8000 as precipitant. The crystals belong to space group $P3_221$, with approximate unit-cell parameters $a = 78.1$, $b = 78.1$, $c = 188.5$ Å, $\alpha = \beta = 90$, $\gamma = 120°$ and a dimer in the asymmetric unit. Test data were collected to beyond 2.6 Å on cryocooled crystals (100 K) using a Rigaku MM007 rotating-anode X-ray source, revealing that the crystals are suitable for a full structural determination.

1. Introduction

Toxoplasma gondii is one of the most widespread infections of man and warm-blooded animals, infecting an estimated 25% of the world's human population (Sibley, 2003). A common transmission route into humans is through the consumption of undercooked contaminated meat and the organism is the third most common cause of food-borne deaths in the United States (Mead *et al.*, 1999). Although commonly asymptomatic, the parasite can produce severe complications and may be fatal. One major risk group is patients suffering from immune suppression, with significant numbers of European and American patients suffering from Acquired Immunodeficiency Syndrome (AIDS) dying from toxoplasmosis (Hill & Dubey, 2002). Another source of severe complications is transmission of *T. gondii* from mother to foetus during pregnancy, which can lead to congenital neurological birth defects (Boyer & McLeod, 2002). Together, the total health care burden within the USA of toxoplasmosis may be up to $5 billion per year (Roberts *et al.*, 1994).

A major hurdle in drug delivery to the intracellular *T. gondii* parasite is the need for the drug to enter the host cell and to cross a vacuolar membrane and the plasma membrane of the parasite. In *T. gondii*, ENR resides within a plastid organelle surrounded by four additional membranes. Drug delivery is made even more difficult in the bradyzoite form of *T. gondii*, which resides in cysts composed of parasite and host constituents. In order to address some of these problems, the common antimicrobial inhibitor triclosan, which has been shown to target and inhibit *T. gondii* enoyl-ACP reductase (TgENR; McLeod *et al.*, 2001), was attached to a releasable octa-arginine linker and the construct was shown to enhance the effectiveness of triclosan as an antiparasitic agent (Samuel *et al.*, 2003).

The structure of ENR has been solved from *Escherichia coli*, *Brassica napus*, *Mycobacterium tuberculosis* and *Plasmodium falciparum*. These structures reveal a common architecture reminiscent of a Rossmann dinucleotide-binding fold, with a parallel β-sheet flanked by α-helices (Rossmann *et al.*, 1974). Furthermore, the structure of

ENR complexed with a range of chemically distinct inhibitors has revealed key areas of the enzyme that are involved in inhibitor binding (Roujeinikova *et al.*, 1999; Qiu *et al.*, 1999; Levy *et al.*, 2001; Miller *et al.*, 2002; Pidugu *et al.*, 2004). Analysis of ENR from *P. falciparum*, a close relative of *T. gondii*, reveals that although the substrate/inhibitor-binding pocket is similar to those of the plant and bacterial enzymes, there are distinct differences which could be exploited for future drug design (Pidugu *et al.*, 2004). Amino-acid sequence analysis of the ENR enzymes from *P. falciparum* and *T. gondii* shows the presence of a low-complexity hydrophilic insert ranging in size from 42 to six amino acids, respectively, which is not mirrored in any plant or bacterial ENR. In order to study the structural consequences of this insert and to develop ENR as a drug target for *T. gondii* therapy, we have initiated a program of rational drug design on TgENR. In this paper, we report the crystallization and preliminary X-ray analysis of TgENR complexed with NAD^+ and triclosan.

2. Materials and methods

2.1. Cloning and overexpression

The coding sequence of *T. gondii* ENR was amplified from cDNA of the RH strain of *T. gondii* (Samuel *et al.*, 2003). The 37-mer forward and reverse primers (forward 5′-GGTGGT**GAATTC**T-CAAACATAAACAAAATTAAAGAAG-3′ and reverse 5′-GGT-GGT**GTCGAC**TTATTCATTTTCATTGCGATATATATC-3′) were used to amplify nucleotides encoding amino-acid residues 103–417 of TgENR and to introduce a proximal *Eco*RI and distal *Sal*I site (bold) into the PCR product. Nucleotides encoding the amino-terminal 102 residues of TgENR were not amplified as they are predicted to encode a signal peptide and an organellar transit peptide. The resulting amplicon was digested with *Eco*RI and *Sal*I and ligated into the pMALc2x vector (New England Biolabs), which produces a fusion protein with the maltose-binding protein (MBP) at the amino-terminus. A second construct of TgENR, also containing residues 103–417, was designed for *in vivo* cleavage by the TEV (tobacco etch

virus) protease. The amplicon described above was ligated into a modified version of the pMALc2x vector (pMALcHT) in which the linker region was altered to contain nucleotides encoding a TEV protease cleavage site followed by a hexahistidine tag (Muench *et al.*, 2003). The resulting ligation product, pSTP8, was transformed into BL21 Star (DE3) cells (Invitrogen) and cotransformed with the pRIL plasmid from BL21-CodonPlus (DE3) cells (Stratagene) and a plasmid encoding the TEV protease (Kapust & Waugh, 2000). Cells were grown in LB medium at 310 K to an optical density at 600 nm of 0.8 and then induced by addition of IPTG to a final concentration of 0.4 mM. The culture was maintained in shaker flasks at 293 K for 12 h to ensure efficient *in vivo* cleavage of the fusion protein by TEV protease and then harvested by centrifugation.

2.2. Purification

Cells were resuspended in lysis buffer [20 mM sodium/potassium phosphate pH 7.5, 1 mg ml^{-1} lysozyme (Sigma), 2.5 µg ml^{-1} DNAse I (Sigma), 20 mM NaCl] and sonicated. The cell lysate was clarified by centrifugation and applied onto a 5 ml HiTrap Chelating HP column (Amersham Biosciences) equilibrated in 20 mM sodium/potassium phosphate pH 7.5, 200 mM NaCl for affinity purification. TgENR was eluted in a linear gradient to 500 mM imidazole at pH 7.5. Column fractions containing cleaved TgENR were desalted with a HiPrep 26/10 desalting column (Amersham Biosciences) equilibrated in 20 mM Tris pH 7.25 and loaded directly onto a 5 ml HiTrap Q Fast Flow column (Amersham Biosciences). Bound proteins were eluted with a linear gradient to 1 M NaCl. Column fractions containing TgENR were pooled and passed through a subtractive 20 ml amylose column (New England Biolabs) to remove any residual uncut fusion protein. Pure TgENR fractions were concentrated to 20 mg ml^{-1} for crystallization trials.

2.3. Crystallization and preliminary X-ray analysis

Initial crystallization trials were carried out at 290 K with Hampton Research Crystal Screens I and II and PEG/Ion Screen using the hanging-drop vapour-diffusion technique, mixing 1.5 µl of 10 mg ml^{-1}
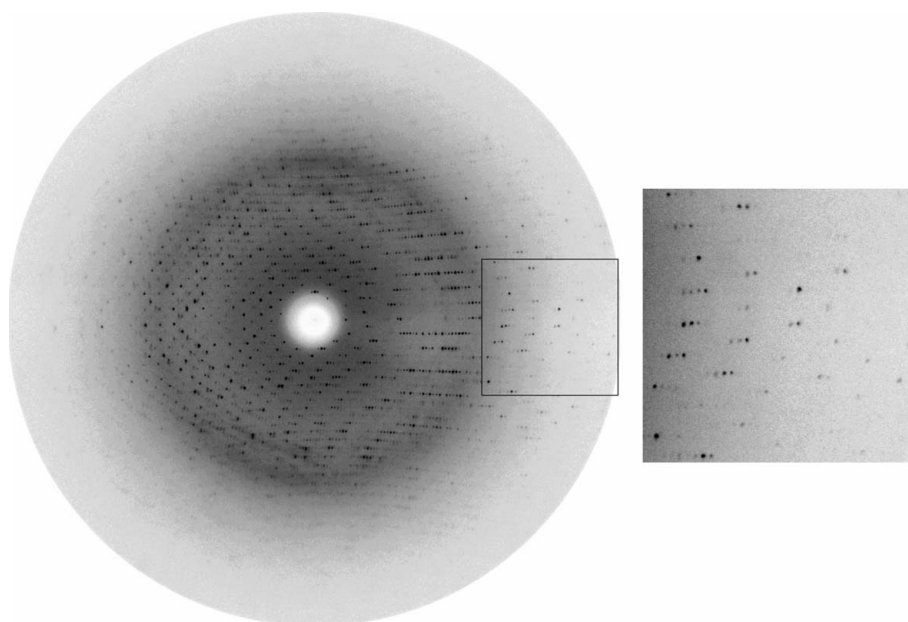

Figure 1
A representative 1° oscillation image of data collected from a TgENR–NAD^+–triclosan complex crystal using a MAR 345 detector mounted on a Rigaku MM007 generator. An enlarged view of the region indicated by a square on the diffraction pattern is shown on the right. The edge of the image corresponds to a resolution of 2.4 Å.

Table 1
Data-collection and processing statistics for TgENR–NAD⁺–triclosan crystals.

Values in parentheses are for the highest resolution shell.

Space group	$P3_221$
Wavelength (Å)	1.54
Resolution (Å)	30–2.6 (2.69–2.6)
Unique reflections	21105
Multiplicity	5.2
Data completeness (%)	99.9 (99.4)
$I/\sigma(I) > 3$ (%)	74.4 (42.0)
R_{merge}† (%)	0.082 (0.48)

† $R_{merge} = \sum_{hkl} |I_i - I_m| / \sum_{hkl} I_i$, where I_i and I_m are the observed intensity and mean intensity of related reflections, respectively.

protein solution (20 mM Tris 7.5 and 100 mM NaCl) and an equivalent volume of reservoir solution. Three sets of crystallization trials were conducted with TgENR in its apo form and in complex with NAD⁺ (5 µM) and with NAD⁺ and triclosan (5 µM NAD⁺ and 6 µM triclosan). Of those conditions which produced crystals, the best quality were those of the TgENR–NAD⁺–triclosan complex, which grew in Crystal Screen 1 condition No. 36 (0.1 M Tris–HCl pH 8.5 and 8% PEG 8000) and reached dimensions of approximately $0.2 \times 0.2 \times 0.3$ mm. Optimization of these conditions led to crystals grown in 0.1 M Tris–HCl pH 9.0 with 6% PEG 8000. For preliminary X-ray analysis, crystals were flash-frozen in 30% glycerol and data were collected at 100 K using an oscillation width of 1° and an exposure time of 10 min on a MAR 345 image-plate detector mounted on a Rigaku MM007 generator. Analysis of the data was carried out using the *DENZO/SCALEPACK* package (Otwinowski & Minor, 1997).

3. Results and discussion

In searching for an appropriate cryoprotectant solution for the crystals of the TgENR–NAD⁺–triclosan complex, 30% glycerol produced promising results; however, this produced a significant increase in mosaicity compared with crystals which were tube-mounted and analysed at room temperature. In order to overcome this problem, crystallization trials were conducted in 0.1 M Tris–HCl pH 9.0 with 6% PEG 8000 and the addition of 5, 10, 15, 20 and 30% glycerol. Crystals of a similar morphology grew in all conditions, although fewer but larger crystals grew in the presence of greater than 15% glycerol. The inclusion of 5% glycerol increased crystal stability during stepwise soaking in 30% glycerol with no significant increase in crystal mosaicity. However, crystals which grew in higher levels of glycerol had much reduced diffraction properties. Crystals grown in the above conditions with an additional 5% glycerol were flash-frozen in 30% glycerol at 100 K and data were collected using a rotation oscillation of 1° and an exposure time of 10 min on a MAR345 image-plate detector mounted on a Rigaku MM007 generator to produce a preliminary data set to 2.6 Å (Fig. 1).

Autoindexing and scaling of the data collected were carried out using *DENZO/SCALEPACK* (Otwinowski & Minor, 1997) and preliminary analysis indicated that the crystals belonged to the trigonal space group *P*321, with unit-cell parameters $a = 78.1$, $b = 78.1$, $c = 188.5$ Å, $\alpha = \beta = 90$, $\gamma = 120°$. Analysis of the systematic absences within the X-ray diffraction pattern revealed the crystals to belong to space group $P3_121$ or $P3_221$. Data-collection and processing statistics can be found in Table 1. Analysis of the V_M for the TgENR–NAD⁺–triclosan crystals suggests that the asymmetric unit contains a dimer, with a V_M of 2.4 Å³ Da⁻¹, which is within the range of V_M values observed for protein crystals (Matthews, 1977). Gel-filtration studies

show that TgENR, like the enzyme from other species, is a tetramer in solution (data not shown) and therefore one of the molecular twofold axes of the tetramer within the asymmetric unit must be coincident with a crystallographic twofold axis.

An initial attempt to solve the structure of TgENR by molecular replacement has been conducted using the program *AMoRe* (Navaza, 1994) with the coordinates of *P. falciparum* ENR (unpublished data) as a search model. The *P. falciparum* ENR search model was edited to remove two loop regions of low sequence similarity (between $\alpha 2$ and $\beta 3$ and between $\beta 3$ and $\alpha 3$) and then split into the three unique combinations of the possible dimer in the asymmetric unit. *AMoRe* provided a convincing solution in space group $P3_221$, but not in $P3_121$, suggesting that the former is the correct space group. Refinement of the structure is currently under way and it is hoped that this may provide a clear insight into the features of the active site that are unique to TgENR and which may be exploited in future drug-development programs.

References

Boyer, K. & McLeod, R. (2002). *Principles and Practice of Paediatric Infectious Diseases*, 2nd ed., edited by S. Long, C. Proeber & L. Pickering, pp. 1303–1322. New York: Churchill Livingstone.
Hill, D. & Dubey, J. P. (2002). *Clin. Microbiol. Infect.* **8**, 634–640.
Kapust, R. B. & Waugh, D. S. (2000). *Protein Expr. Purif.* **19**, 312–318.
Levy, C. W., Baldock, C., Wallace, A. J., Sedelnikova, S., Viner, R. C., Clough, J. M., Stuitje, A. R., Slabas, A. R., Rice, D. W. & Rafferty, J. B. (2001). *J. Mol. Biol.* **309**, 171–180.
McLeod, R., Muench, S. P., Rafferty, J. B., Kyle, D. E., Mui, E. J., Kirisits, M. J., Mack, D. G., Roberts, C. W., Samuel, B. U., Lyons, R. E., Dorris, M., Milhous, W. K. & Rice, D. W. (2001). *Int. J. Parasitol.* **31**, 109–113.
Matthews, B. W. (1977). *X-ray Structure of Proteins*, edited by H. Neurath & R. L. Hill, pp. 468–477. New York: Academic Press.
Mead, P. S., Slutsker, L., Dietz, V., McCaig, L. F., Bresee, J. S., Shapiro, C., Griffin, P. M. & Tauxe, R. V. (1999). *Emerg. Infect. Dis.* **5**, 607–625.
Miller, W. H., Seefeld, M. A., Newlander, K. A., Uzinskas, I. N., Burgess, W. J., Heerding, D. A., Yuan, C. C., Head, M. S., Payne, D. J., Rittenhouse, S. F., Moore, T. D., Pearson, S. C., Berry, V., DeWolf, W. E. Jr, Keller, P. M., Polizzi, B. J., Qiu, X., Janson, C. A. & Huffman, W. F. (2002). *J. Med. Chem.* **45**, 3246–3256.
Muench, S. P., Rafferty, J. B., McLeod, R., Rice, D. W. & Prigge, S. T. (2003). *Acta Cryst.* D**59**, 1246–1248.
Navaza, J. (1994) *Acta Cryst.* A**50**, 157–163.
Otwinowski, Z. & Minor, W. (1997). *Methods Enzymol.* **276**, 307–326.
Pidugu, L. S., Kapoor, M., Surolia, N., Surolia, A. & Suguna, K. (2004). *J. Mol. Biol.* **343**, 147–155.
Qiu, X., Janson, C. A., Court, R. I., Smyth, M. G., Payne, D. J. & Abdel-Meguid, S. S. (1999). *Protein Sci.* **8**, 2529–2532.
Roberts, T., Murrell, K. D. & Marks, S. (1994). *Parasitol. Today*, **10**, 419–423.
Rossmann, M. G., Moras, D. & Olsen, K. W. (1974). *Nature (London)*, **250**, 194–199.
Roujeinikova, A., Sedelnikova, S., de Boer, G. J., Stuitje, A. R., Slabas, A. R., Rafferty, J. B. & Rice, D. W. (1999). *J. Biol. Chem.* **274**, 30811–30817.
Samuel, B. U., Hearn, B., Mack, D., Wender, P., Rothbard, J., Kirisits, M. J., Mui, E., Wernimont, S., Roberts, C. W., Muench, S. P., Rice, D. W., Prigge, S. T., Law, A. B. & McLeod, R. (2003). *Proc. Natl Acad. Sci. USA*, **100**, 14281–14286.
Sibley, L. D. (2003). *Traffic*, **4**, 581–586.